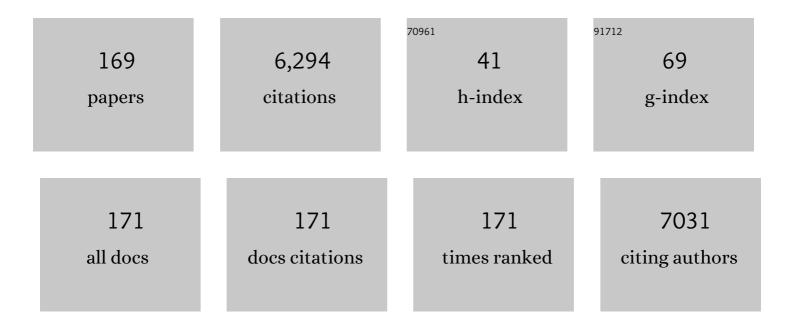
## Seung Soo Lee

List of Publications by Year in descending order

Source: https://exaly.com/author-pdf/5037631/publications.pdf Version: 2024-02-01



#	Article	lF	CITATIONS
1	Crohn Disease of the Small Bowel: Comparison of CT Enterography, MR Enterography, and Small-Bowel Follow-Through as Diagnostic Techniques. Radiology, 2009, 251, 751-761.	3.6	385
2	Radiologic evaluation of nonalcoholic fatty liver disease. World Journal of Gastroenterology, 2014, 20, 7392.	1.4	330
3	Non-invasive assessment of hepatic steatosis: Prospective comparison of the accuracy of imaging examinations. Journal of Hepatology, 2010, 52, 579-585.	1.8	311
4	Visually Isoattenuating Pancreatic Adenocarcinoma at Dynamic-Enhanced CT: Frequency, Clinical and Pathologic Characteristics, and Diagnosis at Imaging Examinations. Radiology, 2010, 257, 87-96.	3.6	212
5	Quantitative analysis of diffusionâ€weighted magnetic resonance imaging of the pancreas: Usefulness in characterizing solid pancreatic masses. Journal of Magnetic Resonance Imaging, 2008, 28, 928-936.	1.9	181
6	Development and Validation of a Deep Learning System for Staging Liver Fibrosis by Using Contrast Agent–enhanced CT Images in the Liver. Radiology, 2018, 289, 688-697.	3.6	153
7	Malignant Hepatic Tumors: Short-term Reproducibility of Apparent Diffusion Coefficients with Breath-hold and Respiratory-triggered Diffusion-weighted MR Imaging. Radiology, 2010, 255, 815-823.	3.6	134
8	LI-RADS Classification and Prognosis of Primary Liver Cancers at Gadoxetic Acid–enhanced MRI. Radiology, 2019, 290, 388-397.	3.6	125
9	CT of Prominent Pericolic or Perienteric Vasculature in Patients with Crohn's Disease: Correlation with Clinical Disease Activity and Findings on Barium Studies. American Journal of Roentgenology, 2002, 179, 1029-1036.	1.0	113
10	Incremental Value of Liver MR Imaging in Patients with Potentially Curable Colorectal Hepatic Metastasis Detected at CT: A Prospective Comparison of Diffusion-weighted Imaging, Gadoxetic Acid–enhanced MR Imaging, and a Combination of Both MR Techniques. Radiology, 2015, 274, 712-722.	3.6	109
11	A Prospective Comparison of Standard-Dose CT Enterography and 50% Reduced-Dose CT Enterography With and Without Noise Reduction for Evaluating Crohn Disease. American Journal of Roentgenology, 2011, 197, 50-57.	1.0	98
12	Hepatic Fat Quantification. Investigative Radiology, 2012, 47, 368-375.	3.5	98
13	Intravoxel Incoherent Motion Diffusion-weighted MR Imaging of the Liver: Effect of Triggering Methods on Regional Variability and Measurement Repeatability of Quantitative Parameters. Radiology, 2015, 274, 405-415.	3.6	93
14	Biopsy-proven Nonsteatotic Liver in Adults: Estimation of Reference Range for Difference in Attenuation between the Liver and the Spleen at Nonenhanced CT. Radiology, 2011, 258, 760-766.	3.6	92
15	Radiomics Analysis of Gadoxetic Acid–enhanced MRI for Staging Liver Fibrosis. Radiology, 2019, 290, 380-387.	3.6	89
16	Non-enhanced magnetic resonance imaging as a surveillance tool for hepatocellular carcinoma: Comparison with ultrasound. Journal of Hepatology, 2020, 72, 718-724.	1.8	86
17	Radiomics and Deep Learning: Hepatic Applications. Korean Journal of Radiology, 2020, 21, 387.	1.5	83
18	Pancreatic Cancer CT: Prediction of Resectability according to NCCN Criteria. Radiology, 2018, 289, 710-718.	3.6	74

#	Article	IF	CITATIONS
19	Intrahepatic Cholangiocarcinoma in Patients with Cirrhosis: Differentiation from Hepatocellular Carcinoma by Using Gadoxetic Acid–enhanced MR Imaging and Dynamic CT. Radiology, 2017, 282, 771-781.	3.6	73
20	Initial human experience of endoscopic ultrasound-guided photodynamic therapy with a novel photosensitizer and a flexible laser-light catheter. Endoscopy, 2015, 47, 1035-1038.	1.0	70
21	MRI Features for Predicting Microvascular Invasion of Hepatocellular Carcinoma: A Systematic Review and Meta-Analysis. Liver Cancer, 2021, 10, 94-106.	4.2	70
22	Obscure Gastrointestinal Bleeding: Diagnostic Performance of Multidetector CT Enterography. Radiology, 2011, 259, 739-748.	3.6	69
23	Intraductal Papillary Neoplasm of the Bile Duct: Clinical, Imaging, and Pathologic Features. American Journal of Roentgenology, 2018, 211, 67-75.	1.0	69
24	Diagnostic performance of CT, gadoxetate disodiumâ€enhanced MRI, and PET/CT for the diagnosis of colorectal liver metastasis: Systematic review and metaâ€analysis. Journal of Magnetic Resonance Imaging, 2018, 47, 1237-1250.	1.9	69
25	Hepatic Arteries in Potential Donors for Living Related Liver Transplantation: Evaluation with Multi–Detector Row CT Angiography. Radiology, 2003, 227, 391-399.	3.6	67
26	Atypical Imaging Features of Primary Central Nervous System Lymphoma That Mimics Glioblastoma: Utility of Intravoxel Incoherent Motion MR Imaging. Radiology, 2014, 272, 504-513.	3.6	67
27	CT colonography for detection and characterisation of synchronous proximal colonic lesions in patients with stenosing colorectal cancer. Gut, 2012, 61, 1716-1722.	6.1	64
28	Reproducibility of measurement of apparent diffusion coefficients of malignant hepatic tumors: Effect of DWI techniques and calculation methods. Journal of Magnetic Resonance Imaging, 2012, 36, 1131-1138.	1.9	62
29	Gadoxetic Acid–enhanced MRI of Hepatocellular Carcinoma: Value of Washout in Transitional and Hepatobiliary Phases. Radiology, 2019, 291, 651-657.	3.6	62
30	Combined hepatocellular-cholangiocarcinoma: Gadoxetic acid-enhanced MRI findings correlated with pathologic features and prognosis. Journal of Magnetic Resonance Imaging, 2017, 46, 267-280.	1.9	59
31	Flat Colorectal Neoplasms: Definition, Importance, and Visualization on CT Colonography. American Journal of Roentgenology, 2007, 188, 953-959.	1.0	57
32	Hepatic fat quantification using chemical shift MR imaging and MR spectroscopy in the presence of hepatic iron deposition: Validation in phantoms and in patients with chronic liver disease. Journal of Magnetic Resonance Imaging, 2011, 33, 1390-1398.	1.9	55
33	Contrast-enhanced computed tomography for the diagnosis of fatty liver: prospective study with same-day biopsy used as the reference standard. European Radiology, 2010, 20, 359-366.	2.3	54
34	Image quality and focal lesion detection on T2-weighted MR imaging of the liver: Comparison of two high-resolution free-breathing imaging techniques with two breath-hold imaging techniques. Journal of Magnetic Resonance Imaging, 2007, 26, 323-330.	1.9	53
35	Intravoxel incoherent motion diffusionâ€weighted MRI of the abdomen: The effect of fitting algorithms on the accuracy and reliability of the parameters. Journal of Magnetic Resonance Imaging, 2017, 45, 1637-1647.	1.9	53
36	CT Colonography for Combined Colonic and Extracolonic Surveillance after Curative Resection of Colorectal Cancer. Radiology, 2010, 257, 697-704.	3.6	52

#	Article	IF	CITATIONS
37	Sensitivity of CT Colonography for Nonpolypoid Colorectal Lesions Interpreted by Human Readers and With Computer-Aided Detection. American Journal of Roentgenology, 2009, 193, 70-78.	1.0	49
38	Intravoxel incoherent motion MRI for liver fibrosis assessment: a pilot study. Acta Radiologica, 2015, 56, 1428-1436.	0.5	47
39	Sclerosing Cholangitis: Clinicopathologic Features, Imaging Spectrum, and Systemic Approach to Differential Diagnosis. Korean Journal of Radiology, 2016, 17, 25.	1.5	46
40	Polyp Measurement Reliability, Accuracy, and Discrepancy: Optical Colonoscopy versus CT Colonography with Pig Colonic Specimens. Radiology, 2007, 244, 157-164.	3.6	44
41	IgG4-related kidney disease: MRI findings with emphasis on the usefulness of diffusion-weighted imaging. European Journal of Radiology, 2014, 83, 1057-1062.	1.2	44
42	Troubleshooting Arterial-Phase MR Images of Gadoxetate Disodium-Enhanced Liver. Korean Journal of Radiology, 2015, 16, 1207.	1.5	43
43	What we need to know when performing and interpreting US elastography. Clinical and Molecular Hepatology, 2016, 22, 406-414.	4.5	43
44	Assessment of liver fibrosis severity using computed tomography–based liver and spleen volumetric indices in patients with chronic liver disease. European Radiology, 2020, 30, 3486-3496.	2.3	42
45	Deep Learning Algorithm for Automated Segmentation and Volume Measurement of the Liver and Spleen Using Portal Venous Phase Computed Tomography Images. Korean Journal of Radiology, 2020, 21, 987.	1.5	40
46	Magnetic Resonance Cholangiopancreatography for the Diagnostic Evaluation of Autoimmune Pancreatitis. Pancreas, 2010, 39, 1191-1198.	0.5	37
47	Diagnostic Strategy for Differentiating Autoimmune Pancreatitis From Pancreatic Cancer. Pancreas, 2012, 41, 639-647.	0.5	37
48	Usefulness of Computed Tomography in Differentiating Transmural Infarction from Nontransmural Ischemia of the Small Intestine in Patients With Acute Mesenteric Venous Thrombosis. Journal of Computer Assisted Tomography, 2008, 32, 730-737.	0.5	36
49	Intrapancreatic Accessory Spleen. Pancreas, 2011, 40, 956-965.	0.5	35
50	Differential diagnosis of sclerosing cholangitis with autoimmune pancreatitis and periductal infiltrating cancer in the common bile duct at dynamic CT, endoscopic retrograde cholangiography and MR cholangiography. European Radiology, 2012, 22, 2502-2513.	2.3	35
51	Diffusion-weighted MRI: usefulness for differentiating intrapancreatic accessory spleen and small hypervascular neuroendocrine tumor of the pancreas. Acta Radiologica, 2014, 55, 1157-1165.	0.5	35
52	Intravoxel incoherent motion diffusion-weighted imaging of the pancreas: Characterization of benign and malignant pancreatic pathologies. Journal of Magnetic Resonance Imaging, 2017, 45, 260-269.	1.9	33
53	CT Colonography after Metallic Stent Placement for Acute Malignant Colonic Obstruction. Radiology, 2010, 254, 774-782.	3.6	32
54	Biologic Factors Affecting HCC Conspicuity in Hepatobiliary Phase Imaging With Liver-Specific Contrast Agents. American Journal of Roentgenology, 2013, 201, 322-331.	1.0	32

#	Article	IF	CITATIONS
55	Hepatic arterial damage after transarterial chemoembolization for the treatment of hepatocellular carcinoma: comparison of drug-eluting bead and conventional chemoembolization in a retrospective controlled study. Acta Radiologica, 2017, 58, 131-139.	0.5	32
56	Comparison of diagnostic performance between CT and MRI in differentiating non-diffuse-type autoimmune pancreatitis from pancreatic ductal adenocarcinoma. European Radiology, 2018, 28, 5267-5274.	2.3	32
57	Estimating Recurrence after Upfront Surgery in Patients with Resectable Pancreatic Ductal Adenocarcinoma by Using Pancreatic CT: Development and Validation of a Risk Score. Radiology, 2020, 296, 541-551.	3.6	32
58	Stereotactic Body Radiotherapy-Induced Arterial Hypervascularity of Non-Tumorous Hepatic Parenchyma in Patients with Hepatocellular Carcinoma: Potential Pitfalls in Tumor Response Evaluation on Multiphase Computed Tomography. PLoS ONE, 2014, 9, e90327.	1.1	31
59	Shear Wave Elastography as a Quantitative Biomarker of Clinically Significant Portal Hypertension: A Systematic Review and Meta-Analysis. American Journal of Roentgenology, 2018, 210, W185-W195.	1.0	31
60	Panoramic endoluminal display with minimal image distortion using circumferential radial ray-casting for primary three-dimensional interpretation of CT colonography. European Radiology, 2009, 19, 1951-1959.	2.3	30
61	Ultrasonographic features of fibrous hamartoma of infancy. Skeletal Radiology, 2014, 43, 649-653.	1.2	30
62	Neoadjuvant modified FOLFIRINOX followed by postoperative gemcitabine in borderline resectable pancreatic adenocarcinoma: a Phase 2 study for clinical and biomarker analysis. British Journal of Cancer, 2020, 123, 362-368.	2.9	29
63	CT-determined resectability of borderline resectable and unresectable pancreatic adenocarcinoma following FOLFIRINOX therapy. European Radiology, 2021, 31, 813-823.	2.3	29
64	Preoperative prediction of postsurgical outcomes in mass-forming intrahepatic cholangiocarcinoma based on clinical, radiologic, and radiomics features. European Radiology, 2021, 31, 8638-8648.	2.3	28
65	Sclerosing cholangitis with autoimmune pancreatitis <i>versus</i> primary sclerosing cholangitis: comparison on endoscopic retrograde cholangiography, MR cholangiography, CT, and MRI. Acta Radiologica, 2013, 54, 601-607.	0.5	27
66	CT indices for the diagnosis of hepatic steatosis using non-enhanced CT images: development and validation of diagnostic cut-off values in a large cohort with pathological reference standard. European Radiology, 2019, 29, 4427-4435.	2.3	27
67	CT Colonography for Follow-Up After Surgery for Colorectal Cancer. American Journal of Roentgenology, 2007, 189, 283-289.	1.0	26
68	Colorectal Polyps on Portal Phase Contrast-Enhanced CT Colonography: Lesion Attenuation and Distinction from Tagged Feces. American Journal of Roentgenology, 2007, 189, 35-40.	1.0	26
69	Intravoxel incoherent motion diffusionâ€weighted imaging for characterizing focal hepatic lesions: Correlation with lesion enhancement. Journal of Magnetic Resonance Imaging, 2017, 45, 1589-1598.	1.9	26
70	Selection and Reporting of Statistical Methods to Assess Reliability of a Diagnostic Test: Conformity to Recommended Methods in a Peer-Reviewed Journal. Korean Journal of Radiology, 2017, 18, 888.	1.5	26
71	A simple score for predicting mortality in patients with pneumatosis intestinalis. European Journal of Radiology, 2014, 83, 639-645.	1.2	25
72	Differentiating focal autoimmune pancreatitis and pancreatic ductal adenocarcinoma: contrast-enhanced MRI with special emphasis on the arterial phase. European Radiology, 2019, 29, 5763-5771.	2.3	25

#	Article	IF	CITATIONS
73	Hypervascular solid-appearing serous cystic neoplasms of the pancreas: Differential diagnosis with neuroendocrine tumours. European Radiology, 2016, 26, 1348-1358.	2.3	24
74	Interreader Agreement of Liver Imaging Reporting and Data System on MRI: A Systematic Review and Metaâ€Analysis. Journal of Magnetic Resonance Imaging, 2020, 52, 795-804.	1.9	24
75	MR Imaging of Reperfused Myocardial Infarction: Comparison of Necrosis-Specific and Intravascular Contrast Agents in a Cat Model. Radiology, 2003, 226, 739-747.	3.6	23
76	Computed Tomography Evaluation of Gastrointestinal Bleeding and Acute Mesenteric Ischemia. Radiologic Clinics of North America, 2013, 51, 29-43.	0.9	23
77	Immunoglobulin G4-Related Kidney Disease: A Comprehensive Pictorial Review of the Imaging Spectrum, Mimickers, and Clinicopathological Characteristics. Korean Journal of Radiology, 2015, 16, 1056.	1.5	23
78	Perfusion Assessment Using Intravoxel Incoherent Motion-Based Analysis of Diffusion-Weighted Magnetic Resonance Imaging. Investigative Radiology, 2016, 51, 520-528.	3.5	23
79	Noninvasive assessment of hepatic sinusoidal obstructive syndrome using acoustic radiation force impulse elastography imaging: A proof-of-concept study in rat models. European Radiology, 2018, 28, 2096-2106.	2.3	23
80	Linear Polyp Measurement at CT Colonography: 3D Endoluminal Measurement with Optimized Surface-rendering Threshold Value and Automated Measurement. Radiology, 2008, 246, 157-167.	3.6	22
81	Atypical Manifestations of IgG4-Related Sclerosing Disease in the Abdomen: Imaging Findings and Pathologic Correlations. American Journal of Roentgenology, 2013, 200, 102-112.	1.0	22
82	Relapse of IgG4-related sclerosing cholangitis after steroid therapy: image findings and risk factors. European Radiology, 2014, 24, 1039-1048.	2.3	22
83	Meta-analysis of the accuracy of Liver Imaging Reporting and Data System category 4 or 5 for diagnosing hepatocellular carcinoma. Gut, 2019, 68, 1719-1721.	6.1	22
84	Superficial Esophageal Cancer: Esophagographic Findings Correlated with Histopathologic Findings. Radiology, 2005, 236, 535-544.	3.6	21
85	Shear Wave Elastography for Assessment of Steatohepatitis andÂHepatic Fibrosis in Rat Models of Non-Alcoholic Fatty LiverÂDisease. Ultrasound in Medicine and Biology, 2015, 41, 3205-3215.	0.7	21
86	Thread sign in biliary intraductal papillary mucinous neoplasm: a novel specific finding for MRI. European Radiology, 2016, 26, 3112-3120.	2.3	21
87	Diagnostic performance of [18F]FDG-PET/MRI for liver metastasis in patients with primary malignancy: a systematic review and meta-analysis. European Radiology, 2019, 29, 3553-3563.	2.3	21
88	Use of Liver Magnetic Resonance Imaging After Standard Staging Abdominopelvic Computed Tomography to Evaluate Newly Diagnosed Colorectal Cancer Patients. Annals of Surgery, 2015, 261, 480-486.	2.1	20
89	Subtraction Images of Gadoxetic Acid–Enhanced MRI: Effect on the Diagnostic Performance for Focal Hepatic Lesions in Patients at Risk for Hepatocellular Carcinoma. American Journal of Roentgenology, 2017, 209, 584-591.	1.0	20
90	Malignant pancreatic serous cystic neoplasms: systematic review with a new case. BMC Gastroenterology, 2016, 16, 97.	0.8	19

#	Article	IF	CITATIONS
91	Abbreviated MRI with optional multiphasic CT as an alternative to full-sequence MRI: LI-RADS validation in a HCC-screening cohort. European Radiology, 2020, 30, 2302-2311.	2.3	19
92	Liver imaging reporting and data system category M: A systematic review and metaâ€analysis. Liver International, 2020, 40, 1477-1487.	1.9	19
93	Deep learning–based algorithm to detect primary hepatic malignancy in multiphase CT of patients at high risk for HCC. European Radiology, 2021, 31, 7047-7057.	2.3	19
94	Radiologic Evaluation and Structured Reporting Form for Extrahepatic Bile Duct Cancer: 2019 Consensus Recommendations from the Korean Society of Abdominal Radiology. Korean Journal of Radiology, 2021, 22, 41.	1.5	19
95	Primary Extrapulmonary Small Cell Carcinoma Involving the Stomach or Duodenum or Both: Findings on CT and Barium Studies. American Journal of Roentgenology, 2003, 180, 1325-1329.	1.0	18
96	Automated Carbon Dioxide Insufflation for CT Colonography: Effectiveness of Colonic Distention in Cancer Patients with Severe Luminal Narrowing. American Journal of Roentgenology, 2008, 190, 698-706.	1.0	18
97	Diffusion-weighted MR enterography for evaluating Crohn's disease: Effect of anti-peristaltic agent on the diagnosis of bowel inflammation. European Radiology, 2017, 27, 2554-2562.	2.3	18
98	Interobserver Reproducibility in Sonographic Measurement of Diameter and Volume of Papillary Thyroid Microcarcinoma. Thyroid, 2021, 31, 452-458.	2.4	18
99	An index based on deep learning–measured spleen volume on CT for the assessment of high-risk varix in B-viral compensated cirrhosis. European Radiology, 2021, 31, 3355-3365.	2.3	18
100	Accuracy of the ultrasound attenuation coefficient for the evaluation of hepatic steatosis: a systematic review and meta-analysis of prospective studies. Ultrasonography, 2022, 41, 83-92.	1.0	18
101	Occlusive Myocardial Infarction: Investigation ofBis-Gadolinium Mesoporphyrins–enhanced T1-weighted MR Imaging in a Cat Model. Radiology, 2001, 220, 436-440.	3.6	17
102	Phagocytic function of Kupffer cells in mouse nonalcoholic fatty liver disease models: Evaluation with superparamagnetic iron oxide. Journal of Magnetic Resonance Imaging, 2015, 41, 1218-1227.	1.9	17
103	Retrospective analysis of current guidelines for hepatocellular carcinoma diagnosis on gadoxetic acid–enhanced MRI in at-risk patients. European Radiology, 2021, 31, 4751-4763.	2.3	17
104	Porto-sinusoidal vascular disease with portal hypertension versus liver cirrhosis: differences in imaging features on CT and hepatobiliary contrast-enhanced MRI. Abdominal Radiology, 2021, 46, 1891-1903.	1.0	16
105	CT in the prediction of margin-negative resection in pancreatic cancer following neoadjuvant treatment: a systematic review and meta-analysis. European Radiology, 2021, 31, 3383-3393.	2.3	16
106	Successful Implementation of an Artificial Intelligence-Based Computer-Aided Detection System for Chest Radiography in Daily Clinical Practice. Korean Journal of Radiology, 2022, 23, 847.	1.5	16
107	Efficacy of Barium-Based Fecal Tagging for CT Colonography: a Comparison between the Use of High and Low Density Barium Suspensions in a Korean Population - a Preliminary Study. Korean Journal of Radiology, 2009, 10, 25.	1.5	15
108	Meta-Analysis of the Accuracy of Abbreviated Magnetic Resonance Imaging for Hepatocellular Carcinoma Surveillance: Non-Contrast versus Hepatobiliary Phase-Abbreviated Magnetic Resonance Imaging. Cancers, 2021, 13, 2975.	1.7	15

#	Article	IF	CITATIONS
109	Contrast-enhanced MR cholangiography with Gd-EOB-DTPA for preoperative biliary mapping: correlation with intraoperative cholangiography. Acta Radiologica, 2015, 56, 773-781.	0.5	14
110	Inflammatory fibroid polyps of the gastrointestinal tract: a 14-year CT study at a single institution. Abdominal Imaging, 2015, 40, 2159-2166.	2.0	14
111	Intravoxel incoherent motion MRI for monitoring the therapeutic response of hepatocellular carcinoma to sorafenib treatment in mouse xenograft tumor models. Acta Radiologica, 2017, 58, 1045-1053.	0.5	14
112	Liver-to-Spleen Volume Ratio Automatically Measured on CT Predicts Decompensation in Patients with B Viral Compensated Cirrhosis. Korean Journal of Radiology, 2021, 22, 1985.	1.5	14
113	Clinical Staging of Massâ€Forming Intrahepatic Cholangiocarcinoma: Computed Tomography Versus Magnetic Resonance Imaging. Hepatology Communications, 2021, 5, 2009-2018.	2.0	14
114	Characterizing Computed Tomography-Detected Arterial Hyperenhancing-Only Lesions in Patients at Risk of Hepatocellular Carcinoma: Can Non-Contrast Magnetic Resonance Imaging Be Used for Sequential Imaging?. Korean Journal of Radiology, 2020, 21, 280.	1.5	14
115	A comparison of enhancement patterns on dynamic enhanced CT and survival between patients with pancreatic neuroendocrine tumors with and without intratumoral fibrosis. Abdominal Radiology, 2017, 42, 2835-2842.	1.0	13
116	Agreement and Reproducibility of Proton Density Fat Fraction Measurements Using Commercial MR Sequences Across Different Platforms. Investigative Radiology, 2019, 54, 517-523.	3.5	13
117	The Liver Imaging Reporting and Data System tumor-in-vein category: a systematic review and meta-analysis. European Radiology, 2021, 31, 2497-2506.	2.3	12
118	Inter-reader reliability of CT Liver Imaging Reporting and Data System according to imaging analysis methodology: a systematic review and meta-analysis. European Radiology, 2021, 31, 6856-6867.	2.3	12
119	Population-based and Personalized Reference Intervals for Liver and Spleen Volumes in Healthy Individuals and Those with Viral Hepatitis. Radiology, 2021, 301, 339-347.	3.6	12
120	Value of CT and Doppler Sonography in the Evaluation of Hepatic Vein Stenosis After Dual-Graft Living Donor Liver Transplantation. American Journal of Roentgenology, 2007, 189, 101-108.	1.0	11
121	Migration of Internal Pancreaticojejunostomy Stents into the Bile Ducts in Patients Undergoing Pancreatoduodenectomy. Journal of Gastrointestinal Surgery, 2015, 19, 1995-2002.	0.9	11
122	Real-time two-dimensional Shear-wave elastography for liver stiffness in children: Interobserver variation and effect of breathing technique. European Journal of Radiology, 2017, 97, 53-58.	1.2	11
123	Clinical impact of preoperative liver MRI in the evaluation of synchronous liver metastasis of colon cancer. European Radiology, 2018, 28, 4234-4242.	2.3	11
124	Diagnostic performance of MRI for HCC according to contrast agent type: a systematic review and meta-analysis. Hepatology International, 2020, 14, 1009-1022.	1.9	11
125	Volume Rendering with Color Coding of Tagged Stool during Endoluminal Fly-through CT Colonography: Effect on Reading Efficiency. Radiology, 2008, 248, 1018-1027.	3.6	10
126	Ascending colon rotation following patient positional change during CT colonography: a potential pitfall in interpretation. European Radiology, 2011, 21, 353-359.	2.3	10

#	Article	IF	CITATIONS
127	CT Colonography in Patients Who Have Undergone Sigmoid Colostomy: A Feasibility Study. American Journal of Roentgenology, 2011, 197, W653-W657.	1.0	10
128	MRI Findings and Prediction of Time to Progression of Patients with Hepatocellular Carcinoma Treated with Drug-eluting Bead Transcatheter Arterial Chemoembolization. Journal of Korean Medical Science, 2015, 30, 965.	1.1	10
129	Stiffness of the Central Corpus Cavernosum on Shear-Wave Elastography Is Inversely Correlated with the Penile Rigidity Score in Patients with Erectile Dysfunction. World Journal of Men?s Health, 2021, 39, 123.	1.7	10
130	Systematic review and meta-analysis of diagnostic performance of CT imaging for assessing resectability of pancreatic ductal adenocarcinoma after neoadjuvant therapy: importance of CT criteria. Abdominal Radiology, 2021, 46, 5201-5217.	1.0	10
131	Gadobenate dimeglumineâ€enhanced liver MR imaging in cirrhotic patients: Quantitative and qualitative comparison of 1â€hour and 3â€hour delayed images. Journal of Magnetic Resonance Imaging, 2011, 33, 889-897.	1.9	9
132	Comparison between CT Colonography and Double-Contrast Barium Enema for Colonic Evaluation in Patients with Renal Insufficiency. Korean Journal of Radiology, 2012, 13, 290.	1.5	9
133	Solid Pancreatic Tumors with Unilocular Cyst-Like Appearance on CT: Differentiation from Unilocular Cystic Tumors Using CT. Korean Journal of Radiology, 2014, 15, 704.	1.5	9
134	Primitive Neuroectodermal Tumor of the Stomach. International Journal of Surgical Pathology, 2016, 24, 543-547.	0.4	9
135	Hepatic Safety of Febuxostat Compared with Allopurinol in Gout Patients with Fatty Liver Disease. Journal of Rheumatology, 2019, 46, 527-531.	1.0	9
136	Combined <scp>Hepatocellularâ€Cholangiocarcinoma</scp> : Magnetic Resonance Imaging Features and Prognosis According to Risk Factors for Hepatocellular Carcinoma. Journal of Magnetic Resonance Imaging, 2021, 53, 1803-1812.	1.9	9
137	Radiomics and deep learning in liver diseases. Journal of Gastroenterology and Hepatology (Australia), 2021, 36, 561-568.	1.4	9
138	Deep Learning-Based Assessment of Functional Liver Capacity Using Gadoxetic Acid-Enhanced Hepatobiliary Phase MRI. Korean Journal of Radiology, 2022, 23, .	1.5	9
139	Reproducibility of hepatic MR elastography across field strengths, pulse sequences, scan intervals, and readers. Abdominal Radiology, 2020, 45, 107-115.	1.0	8
140	Multiparametric MRI for prediction of treatment response to neoadjuvant FOLFIRINOX therapy in borderline resectable or locally advanced pancreatic cancer. European Radiology, 2021, 31, 864-874.	2.3	8
141	Radio-pathologic correlation of biphenotypic primary liver cancer (combined hepatocellular) Tj ETQq1 1 0.78431 liver MRI. European Radiology, 2021, 31, 9479-9488.	4 rgBT /O 2.3	verlock 10 Tf. 8
142	Cytomegalovirus Enterocolitis in Apparently Immunocompetent Hosts. Journal of Computer Assisted Tomography, 2010, 34, 892-898.	0.5	7
143	Parallel imaging improves the image quality and duct visibility of breathhold twoâ€dimensional thickâ€slab MR cholangiopancreatography. Journal of Magnetic Resonance Imaging, 2014, 39, 269-275.	1.9	7
144	Prediction of transarterial chemoembolization refractoriness in patients with hepatocellular carcinoma using imaging features of gadoxetic acid-enhanced magnetic resonance imaging. Acta Radiologica, 2021, 62, 1548-1558.	0.5	7

#	Article	IF	CITATIONS
145	Preoperative magnetic resonance imagingâ€based prognostic model for massâ€forming intrahepatic cholangiocarcinoma. Liver International, 2022, 42, 930-941.	1.9	7
146	Impact of the Liver Imaging Reporting and Data System on Research Studies of Diagnosing Hepatocellular Carcinoma Using MRI. Korean Journal of Radiology, 2022, 23, 529.	1.5	7
147	Pancreatic Duct in Autoimmune Pancreatitis. Pancreas, 2017, 46, 921-926.	0.5	6
148	The Effects of Breathing Motion on DCE-MRI Images: Phantom Studies Simulating Respiratory Motion to Compare CAIPIRINHA-VIBE, Radial-VIBE, and Conventional VIBE. Korean Journal of Radiology, 2017, 18, 289.	1.5	6
149	Effectiveness of early endoscopic ultrasound-guided drainage for postoperative fluid collection. Surgical Endoscopy and Other Interventional Techniques, 2022, 36, 135-142.	1.3	6
150	Diagnostic performance of ultrasonography-guided core-needle biopsy according to MRI LI-RADS diagnostic categories. Ultrasonography, 2021, 40, 387-397.	1.0	6
151	Magnetic Resonance Imaging for Surveillance of Hepatocellular Carcinoma: A Systematic Review and Meta-Analysis. Diagnostics, 2021, 11, 1665.	1.3	6
152	Development and Validation of a Simple Index Based on Non-Enhanced CT and Clinical Factors for Prediction of Non-Alcoholic Fatty Liver Disease. Korean Journal of Radiology, 2020, 21, 413.	1.5	6
153	Clinical usefulness of multiple arterial-phase images in gadoxetate disodium-enhanced magnetic resonance imaging: a systematic review and meta-analysis. European Radiology, 2022, 32, 5413-5423.	2.3	6
154	Accuracy and Efficiency of Right-Lobe Graft Weight Estimation Using Deep-Learning-Assisted CT Volumetry for Living-Donor Liver Transplantation. Diagnostics, 2022, 12, 590.	1.3	6
155	Assessment of Measurement Repeatability and Reliability With Virtual Touch Tissue Quantification Imaging in Cervical Lymphadenopathy. Journal of Ultrasound in Medicine, 2016, 35, 927-932.	0.8	5
156	Comparison of CAIPIRINHA-VIBE, Radial-VIBE, and conventional VIBE sequences for dynamic contrast-enhanced (DCE) MRI: A validation study using a DCE-MRI phantom. Magnetic Resonance Imaging, 2016, 34, 638-644.	1.0	5
157	Imaging and clinical features of xanthogranulomatous pancreatitis: an analysis of 10 cases at a single institution. Abdominal Radiology, 2018, 43, 3349-3356.	1.0	5
158	Imaging Patterns of Bacillus Calmette–Guérin-Related Granulomatous Prostatitis Based on Multiparametric MRI. Korean Journal of Radiology, 2022, 23, 60.	1.5	5
159	Effect of Respiration on the Spectral Doppler Wave of the Right Hepatic Vein in Right Lobe Living Donor Liver Transplant Recipients. Journal of Ultrasound in Medicine, 2007, 26, 1723-1733.	0.8	4
160	Feasibility of non-enhanced CT for assessing longitudinal changes in hepatic steatosis. Medicine (United States), 2019, 98, e15606.	0.4	3
161	Adenomatous Neoplasia: Postsurgical Incidence after Normal Preoperative CT Colonography Findings in the Colon Proximal to an Occlusive Cancer. Radiology, 2014, 273, 99-107.	3.6	1
162	Growth rate of serous pancreatic neoplasms inÂvivo: a retrospective, observational study. Acta Radiologica, 2019, 60, 433-440.	0.5	1

#	Article	IF	CITATIONS
163	Development of a multi-channel NIRS-USG hybrid imaging system for detecting prostate cancer and improving the accuracy of imaging-based diagnosis: a phantom study. Ultrasonography, 2019, 38, 143-148.	1.0	1
164	Value of apparent diffusion coefficient for differentiating peripancreatic tuberculous lymphadenopathy from metastatic lymphadenopathy. Abdominal Radiology, 2020, 45, 3163-3171.	1.0	1
165	Imaging of Scrotal Tumors. Journal of the Korean Society of Radiology, 2021, 82, 1053.	0.1	1
166	Differentiation Between Hepatocellular Carcinoma and Colorectal Cancer Liver Metastases on High-Resolution Magic Angle Spinning Spectroscopy: Preliminary Study. Applied Magnetic Resonance, 2014, 45, 19-35.	0.6	0
167	The Significance of Beaking Sign on Cystography in Stress Urinary Incontinence. Journal of the Korean Radiological Society, 2001, 45, 405.	0.0	0
168	Usefulness of CT in Assessing Disease Activity of Crohn's Disease. Journal of the Korean Radiological Society, 2001, 45, 373.	0.0	0
169	Phase II trial of preoperative modified FOLFIRINOX (mFOLFIRINOX) followed by postoperative gemcitabine (GEM) in patients (pts) with borderline resectable pancreatic ductal adenocarcinomas (BR-PDAC) Journal of Clinical Oncology, 2019, 37, 342-342.	0.8	0